

# Electric Driven Molecular Switching of Asymmetric Tris(phthalocyaninato) Lutetium Triple-Decker Complex at the Liquid/Solid Interface

Sheng-Bin Lei,<sup>†</sup> Ke Deng,<sup>†</sup> Yan-Lian Yang,<sup>†</sup> Qing-Dao Zeng,<sup>†</sup> Chen Wang,<sup>\*,†</sup> and Jian-Zhuang Jiang<sup>\*,‡</sup>

*National Center for Nanoscience and Technology, Beijing 100080, People's Republic of China, and Department of Chemistry, Shandong University, Jinan, 250100, China*

*Received February 1, 2008; Revised Manuscript Received April 21, 2008*

## ABSTRACT

Molecular structures are known to significantly impact the adsorption and assembling behavior of the adsorbates on surfaces. Precise control of the molecular orientation and ordering will enable us to tailor the physical and chemical properties of the molecular architectures. In this work, we present a strategy of attaching functional groups with dissimilar adsorption and assembling characteristics to the top and bottom phthalocyaninato moieties of a triple-decker complex, and orientational-dependent ordering of such molecules at the liquid/solid interface has been identified, which is attributed to the interaction of the intrinsic molecular dipole with the external electric field. In addition, isomerization of the noncentrosymmetric tris(phthalocyaninato) lutetium triple-decker complex has been revealed directly with STM and further confirmed by theoretical simulation. This approach provides a possible way for the preparation of organic films with switchable electronic and/or interface properties with external field.

The family of phthalocyanines (Pcs) represents one of the promising candidates for ordered organic thin films in organic electronics due to their significant chemical stability and electronic properties. An important advantage for this class of substance is that both p- and n-type conductivity can be attained by chemical modifications; this is of special importance for realization of complementary logic circuits.<sup>1</sup> Because of the intramolecular interactions and the intrinsic nature of the metal centers, sandwich-type double- and triple-decker complexes of Pcs display characteristic features that cannot be found in their nonsandwich counterparts and which enable them to be used in different areas such as electrochromic displays,<sup>2</sup> field-effect transistors,<sup>3</sup> and gas sensors.<sup>4</sup> For most of the applications, the properties of the molecular devices are closely related to the structure of the solid films. The study of fabrication techniques for a highly ordered film is therefore of great interest for molecular electronics and photonics. Precise control of the molecular orientation and position in an ordered thin film will enable us to tailor the physical and chemical properties of the film. In this work, the assembling structures of an asymmetric triple-decker sandwich complex on the liquid/solid interface have been

studied by scanning tunneling microscopy (STM). Submolecular resolution has been achieved. Interestingly, a bias-induced order-to-disorder phase transition has been observed.

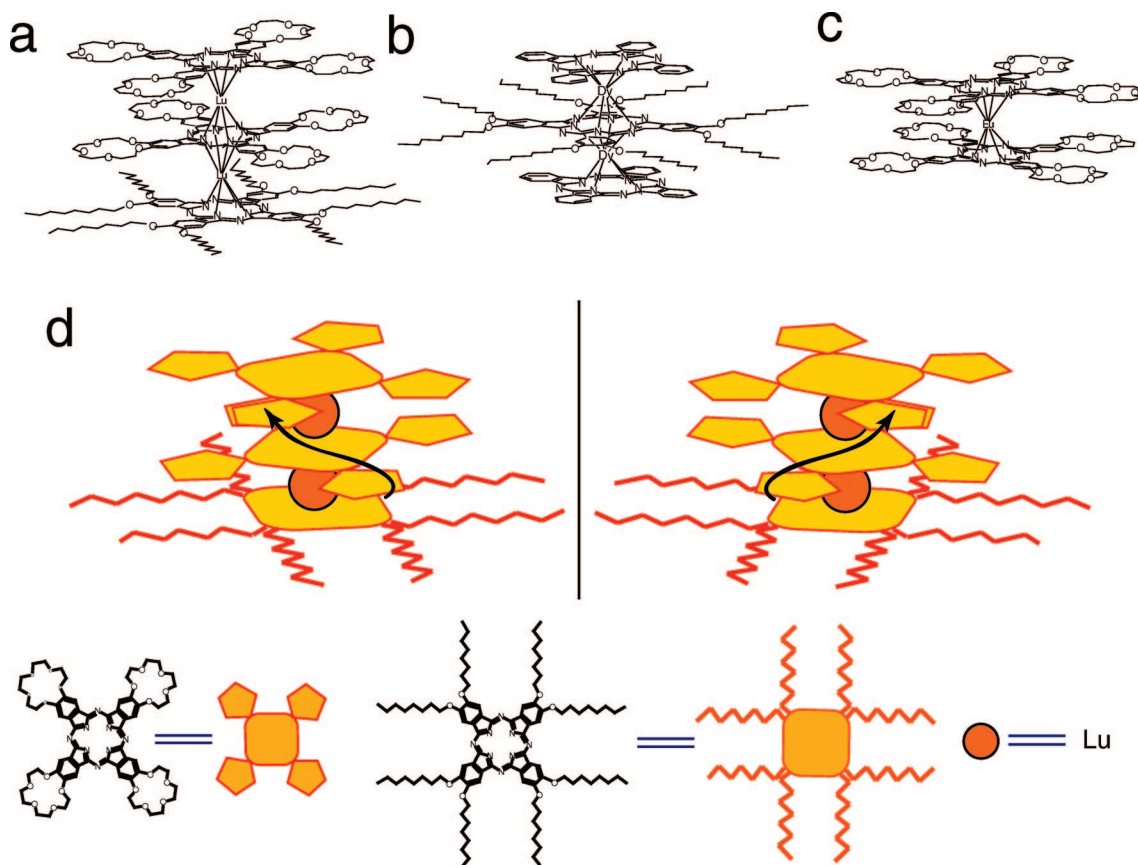
In relation to a possible  $\pi$ -electronic interaction between the two facing phthalocyanine moieties, the relative rotational twisting characteristics of ligand for metal liganded sandwich-type double- and triple-decker complexes are interesting. The rotation can be controlled by coordination to specific functional groups within the molecule, by introducing bulky substituents to the ligands, or by the redox properties of the rare-earth central metal.<sup>5,6</sup> These properties enable the design of a molecular device such as a surface mounted molecular roter based on the controllable rotation of ligand in such kind of sandwich complex.<sup>7</sup> By suppressing the rotation and reducing the symmetry of the ligand, chirality could also be tuned in the sandwich complexes. While monomeric chiral porphyrin and phthalocyanine derivatives have received increasing research interests in the past years,<sup>8</sup> chiral, sandwich-type complexes, especially triple-decker sandwich complexes, still remain rare.<sup>9</sup> Direct observation of molecular chirality by STM has been successful for many species.<sup>10</sup> Though several reports have appeared recently for the STM study of sandwich complexes,<sup>11</sup> no chirality has been directly observed, possibly because of either the low resolution or

\* Corresponding author. E-mail: wangch@nanoctr.cn (C.W.) and jzjiang@sdu.edu.cn (J.-Z.J.).

<sup>†</sup> National Center for Nanoscience and Technology.

<sup>‡</sup> Shandong University.

**Scheme 1.** Molecular Structures of the Noncentrosymmetric and Centrosymmetric Triple-Decker Sandwich Complexes  $[\{Pc(15C5)_4\}Lu\{Pc(15C5)_4\}Lu(PcOC8)]$  (**cpd 1**) (a) and  $[(Pc)Dy(PcOC8)Dy(Pc)]$  (**cpd 2**) (b) Together with the Double-Decker Complex  $Eu[Pc(15C5)_4]_2$  (**cpd 3**) (c), and Schematic Illustration (d) of the Chiral Isomerization of **cpd 1** by Twisting of the Pc Moieties



the small difference of rotation angle between the two isomers.

In comparison with their monophthalocyanine counterparts, the assembling of the sandwich complex is more challenging because of its nonplanar characteristics.<sup>11</sup> Unlike the disk-like (planar) monophthalocyanine, the triple-decker sandwich complex is cylindrical rather than disk-like in apparent shape with its thickness reaching nearly 1 nm, comparable to the lateral size of the phthalocyanine ring (1.3 nm). In this work, our aim is to assemble such triple-decker sandwich complexes into long-range ordered arrays and try to control the ordering in the adlayer by external stimulations. The strategy is by attaching substituents of different polarity to the top or bottom phthalocyaninato moieties, intramolecular charge separation could be induced and subsequently strong intrinsic molecular dipole could be generated. When deposited on the solid surface, such a molecule is expected to show orientational responses to the applied electric field between the STM tip and the substrate.<sup>12</sup> In addition, because of the difference in adsorption and assembling properties of the differently substituted Pc moieties, the change in molecular orientation is expected to cause changes in assembling structure, such as ordering and symmetry. To confirm our concept, two triple-decker sandwich complexes,  $[\{Pc(15C5)_4\}Lu\{Pc(15C5)_4\}Lu(PcOC8)]$  (later on denoted as **cpd 1**) and  $[(Pc)Dy(PcOC8)Dy(Pc)]$  (**cpd 2**), with either noncentrosymmetric or centrosymmetric structure, were synthesized. The

molecular structure of the triple-decker complexes are shown in Scheme 1.<sup>13</sup>

Due to the high electric affinity of the oxygen atoms, the attachment of 15-crown-5 moieties to the Pc ring is expected to cause charge separation in the molecule, where the 15-crown-5 substituted Pc ( $Pc(15C5)_4$ ) moiety is negatively charged and the bottom 2,3,9,10,16,17,23,24-octakis(octyloxy)-phthalocyanine ( $PcOC8$ ) moiety is positively charged. Theoretical calculation using density functional theory (DFT) provided by the DMol3 code have been performed to estimate the magnitude of the molecular dipole.<sup>14</sup> Our simulation reveals a strong intrinsic molecular dipole reaching 17.5 D along the  $z$  axis for the noncentrosymmetric **cpd 1**. Because of the centrosymmetric structure, there is no molecular dipole for **cpd 2**. The 17.5 D molecular dipole is much stronger than that of the nonplanar tin-naphthalocyanine ( $SnNc$ ; 1.48 D), which was reported to exhibit voltage induced flip on the surface.<sup>15</sup> Thus, our sandwich complex is expected to show better responses to the external electric field. The different assembling behavior and affinity to the graphite surface of the  $PcOC8$  and  $Pc(15C5)_4$  moiety is expected to cause different assembling structures for this molecule, so that can serve as an indicator of the electrically induced orientational variation.

STM observations reveal large areas of ordered assembling structure for the noncentrosymmetric **cpd 1** at the 1-phenyloctane/graphite interface under an applied bias ranging from  $-0.30$

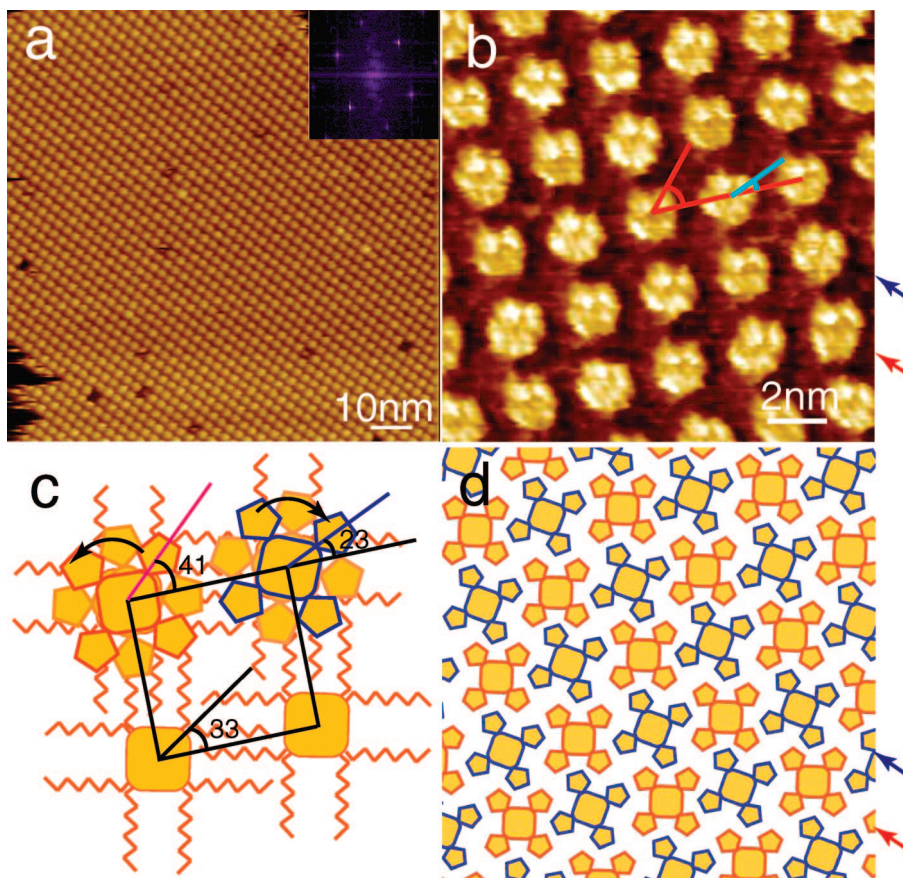


**Figure 1.** Large scale and high resolution STM images obtained on ordered assembling monolayer of **cpd 1** revealed under negative bias (a,b; bias,  $-0.50$  V; tunneling current,  $362$  pA). Two different orientations can be clearly observed from the submolecularly resolved image (as marked by the red and blue arrow in b). The azimuthal angle of the molecules are marked in the image and the definition of azimuthal angle is shown in (c); the azimuthal angle of the top  $Pc(15C5)_4$  and the bottom  $PcOC8$  are shown. Note the unit cell marked here is a fake one in order to facilitate comparison with the monophthalocyanine. (d) A schematic illustration of the molecular packing, only the top  $Pc(15C5)_4$  moiety is shown. The differently orientated molecules are highlighted by different colors in periphery.

to  $-1.50$  V (Figure 1a). Well-ordered domains could extend to hundreds of nanometers at the interface. Different from the former observation on mono- and double-decker phthalocyanine compounds,<sup>11,16</sup> only fourfold symmetric arrangement is observed. The Fourier transform of the image shows clear fourfold symmetry, and the intermolecular distance estimated from the STM image is about  $2.6$  nm, in good consistence with the former observation on monophthalocyanine  $CuPcOC8$  assembly,<sup>16</sup> clearly indicating that **cpd 1** adapts a face-on adsorption configuration with the  $PcOC8$  moiety facing toward the graphite surface and the octyloxy groups fully interdigitated with that from the neighboring molecules. If it adsorbs with the  $Pc(15C5)_4$  facing toward the surface, a  $2.3$  nm intermolecular distance is expected, similar to that of  $Eu[Pc(15C5)_4]_2$  (**cpd 3**; see below). This observation serves as a clear indication that alkylation of the triple-decker structure is effective in stabilizing the adsorbed molecular assemblies at the interface.<sup>16</sup>

In the submolecularly resolved images (Figure 1b), the conjugated phthalocyanine core appears as a four-leaf protrusion with a side length of about  $1.6$  nm. This value is in good consistence with the observation on  $CuPcOC8$  monophthalocyanine ( $1.5$  nm), indicating that only the conjugated  $Pc$  moiety contributes to the bright feature.

Interestingly, the submolecularly resolved STM images clearly indicate that **cpd 1** exhibits discernible orientational differences in the assembled monolayer (Figure 1b). The molecules arranged in a chessboard manner: in the lattice, neighboring molecules rotated for about  $18^\circ$  with respect to each other. The red and blue arrows in Figure 1b mark the differently orientated molecules. The azimuthal angles<sup>17</sup> of the differently orientated molecules are measured to be  $23 \pm 3^\circ$  and  $41 \pm 3^\circ$ , respectively, as illustrated in Figure 1c. The assembling behavior is illustrated in Figure 1d, showing that the alternating molecular rows consisted of molecules with the same twisting characteristics. The molecules with orange colored periphery represent the ones with an azimuthal angle of  $41 \pm 3^\circ$ , while the blue colored one represents molecules with an azimuthal angle of  $23 \pm 3^\circ$ .

The exact same intermolecular distance and symmetry of the two-dimensional (2D) lattice of **cpd 1** with that of  $CuPcOC8$  clearly indicate that the octyloxy chains of the  $PcOC8$  moiety are fully interdigitated; therefore, the bottom  $PcOC8$  moieties have only one possible orientation in the crystal domain. Thus, the different orientations observed in the assembly are most probably due to the twisting of the  $Pc(15C5)_4$  ligands with respect to the  $PcOC8$  moiety.



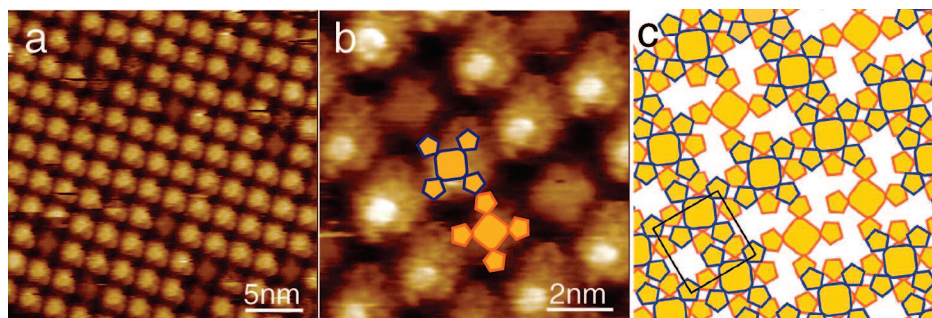


**Figure 2.** Assembly of **cpd 3** at the interface of phenyloctane/graphite. Molecules with lower contrast could be observed both in the large scale (a) and in the high resolution (b) images and are attributed to  $Pc(15C5)_4$  monomers. The orientation of monomer and **cpd 3** could be clearly identified in the high resolution image and indicated with schematic model with orange and blue periphery, respectively. (c) Schematic illustration of the molecular packing correspond to image (b). Imaging condition: bias  $-1.20$  V, tunneling current  $50$  pA.

In order to understand the origination of the different molecular orientations in the lattice of **cpd 1**, the assembling structure of **cpd 3** is studied. Figure 2 shows the assembling structure of **cpd 3**. This compound assembles into well-defined 2D crystalline domains at the liquid/solid interface with fourfold symmetry. From the high resolution STM image (Figure 2b), all of the molecules are aligned with the same azimuthal angle in the lattice. Noticeably, sporadic distributed defects (molecules appear with lower contrast) are observed in the image; we attribute these defects to the residue  $Pc(15C5)_4$  monomers that were coadsorbed with **cpd 3**. By considering the ordering of the lattice, it is reasonable to assume these monomers have the same orientation with the bottom  $Pc(15C5)_4$  moiety of the neighboring **cpd 3** molecules. As demonstrated by previous STM observations on sandwich type molecules,<sup>11,18</sup> commonly, the top Pc ligand (here the top  $Pc(15C5)_4$  moiety) makes a dominant contribution to the image contrast. Thus, by comparing the orientation of **cpd 3** and  $Pc(15C5)_4$  monomers, the relative orientation between the two  $Pc(15C5)_4$  moieties in one **cpd 3** molecule could be determined (Figure 2b). From the high resolution image, the top  $Pc(15C5)_4$  is estimated to rotate for  $45 \pm 3^\circ$  with respect to the bottom one. This result is in line with the reported XRD characterization of heteroleptic  $Eu(Pc)[Pc(15C5)_4]$ , in which a twisting angle of  $44.9^\circ$  is determined.<sup>19</sup>

From the image, the intermolecular distance between **cpd 3** molecules is estimated to be  $2.3 \pm 0.2$  nm, slightly smaller than that of **cpd 1**. According to our previous report and experimental observations, in the fourfold 2D assembly, all of the  $CuPcOC8$  monophthalocyanine molecules show the same orientation with an azimuthal angle of  $33 \pm 3^\circ$  (Figure S2 in Supporting Information).

X-ray diffraction analysis reveals that the orientation of neighboring phthalocyanine moieties in the double- and triple-decker sandwich molecule typically twisted with an angle from  $41$  to  $47^\circ$ , depending on the central metal ion and structure of Pc ligands.<sup>13</sup> This twist of the ligands could induce chiral isomerization to the double-decker sandwich molecules. For triple-decker complexes, the isomerization could even be complex. However, if the two  $Pc[15C5]_4$  ligands in **cpd 1** also orientate with nearly exact  $45^\circ$  orientation as in **cpd 3**, the isomerization will be more

simplified. For the current triple-decker compound, because of the difficulty in obtaining large enough crystals, its structure could not be determined from XRD. Thus, we carried out theoretical simulations using density functional theory (DFT) provided by the DMol3 code.<sup>14</sup> Our simulation shows that in the most stable conformation the top  $Pc(15C5)_4$  ring is orientated with an angle of exactly  $45^\circ$  to the middle  $Pc(15C5)_4$  in the stable conformation, in good agreement with our observation on **cpd 3**. However, the  $PcOC8$  moiety is orientated either  $12^\circ$  larger or  $8^\circ$  smaller than  $45^\circ$  with respect to the middle  $Pc(15C5)_4$  ring and leads to two rotational isomers. The azimuthal angle determined from the STM images indicates the top  $Pc(15C5)_4$  moiety makes a dominant contribution to the image contrast, since a larger azimuthal angle should be expected if the contribution is mainly from the central  $Pc(15C5)_4$  moiety. This is in line with the very recent reports on submolecular STM investigation of double- and triple-decker sandwich complexes.<sup>11,18</sup> From the measured azimuthal angle, the top  $Pc(15C5)_4$  moiety is determined to twist about  $10^\circ$  with respect to the bottom  $PcOC8$  moiety clockwise or  $8^\circ$  counter-clockwise in the isomer, with good agreement to our simulations. The slight asymmetric rotation of these isomers may be caused by the conformation of the 15-crown-5 moieties, for which “chair” conformation is the most stable conformation. Because of the flexibility of these 15-crown-5 moieties, the two isomers are pseudoaxialchiral rather than chiral. According to the STM observation and theoretical simulation, **cpd 1** should be a racemic mixture of two pseudoaxialchiral isomers. The high resolution STM image clearly demonstrates that these molecules form a well-ordered “hetero-chiral” mixture other than phase separation at the liquid/solid interface.

In contrast to the highly ordered domains observed under negative bias, a disordered assembling characteristic is observed at the interface when a positive bias is applied (Figure 3a,b). Submolecular resolution can also be obtained on this disordered layer. Because of the lack of long-range ordering, precise determination of the intermolecular distance is difficult in this assembly. Nevertheless, the intermolecular distance can still be estimated from the FFT of the STM image to be in the range of  $2.3$  to  $2.8$  nm. The submolecular resolution obtained on this disordered layer of **cpd 1** is rather

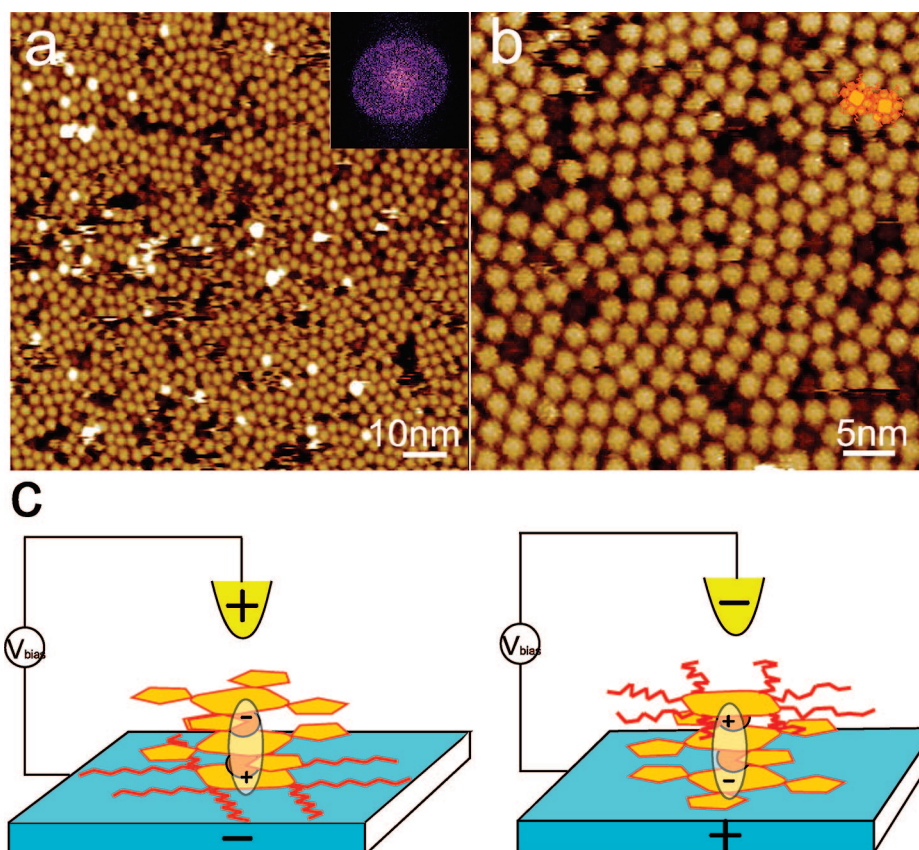


**Figure 3.** Amorphous monolayer structure revealed under positive bias (a,b; bias, 1.50 V; tunneling current, 362 pA.). (c) Schematic illustration of the possible mechanism of the bias induced flipping of the complex. A schematic model is overlaid in (b), with the highlighted squares representing the *Pc* rings of the top *PcOC8* moiety.

surprising since usually submolecular resolution could only be obtained on close packed crystalline domain at the liquid/solid interface. The interaction between the molecular dipole and the applied electric field may at least partially be responsible for the stability of this amorphous structure, since under positive bias the molecule is expected to adsorb with the *Pc*[15C5]<sub>4</sub> moiety toward the surface. In the disordered assembling structure, the *PcOC8* is expected to be away from the substrate toward the solution, and interdigitation of octyloxy groups is unlikely. Therefore, a disordered conformation seems more rational (Figure 3b,c).

An interesting observation is that our experiment reveals the assembling structure of the noncentrosymmetric **cpd 1** could be reversibly switched between order and disorder by changing bias polarity. A typical switching process is shown in Figure 4. Initially, a disordered monolayer of **cpd 1** is revealed under positive bias (Figure 4a). FFT of the image shows typical amorphous characteristic of dispersed ring. However, as the bias is changed to negative, the disordered structure almost immediately transforms into ordered domains with fourfold symmetry (Figure 4b). Consecutive scans under negative bias make the differently orientated domains join together to form a large single domain (Figure 4c–h). At this time, if the bias is switched to positive again (Figure 4i), the long-range ordered assembly could reversibly turn into disordered structure accordingly (Figure 4i–l). At the beginning of this transition process, the ordered domains can still be revealed in some area (Figure 4i,j). While in other

areas, the molecules become non-observable. This may indicate desorption of the molecules from the surface or enhanced mobility of the molecules during orientational changes. In contrast to the fast response (about 2 s) of disorder-to-order transition, the order-to-disorder transition may last for 2 to 3 min.

As noted before, the octyloxy chains of *PcOC8* will fully interdigitate when adsorbed on graphite surface. Because of the high affinity of the octyloxy groups to the graphite surface and strong interaction induced by octyloxy interdigitation, the assembling structure is expected to be rather stable when adsorbed with the *PcOC8* moiety facing toward the surface under negative bias. On the other hand, when adsorbed with the *Pc*(15C5)<sub>4</sub> facing toward the surface under positive bias, no interdigitation will happen. Also, the low affinity of the polar 15-crown-5 substituents to the graphite surface will reduce the stability of the molecule. This could account for the different response speed for the ordering transition to the positive and negative bias. It is also worth noting that the ordered assembling structure could be observed with a rather wide range of bias, ranging from  $-0.30$  to  $-1.50$  V, with the best resolution obtained around  $-0.50$  V. While the stable range of the disordered structure is relatively narrower, from about  $0.80$  to  $1.50$  V, with the best resolution usually obtained under  $1.50$  V. By considering the different assembling characteristics and affinity to the surface of the *PcOC8* and *Pc*(15C5)<sub>4</sub> moieties, this difference in stability



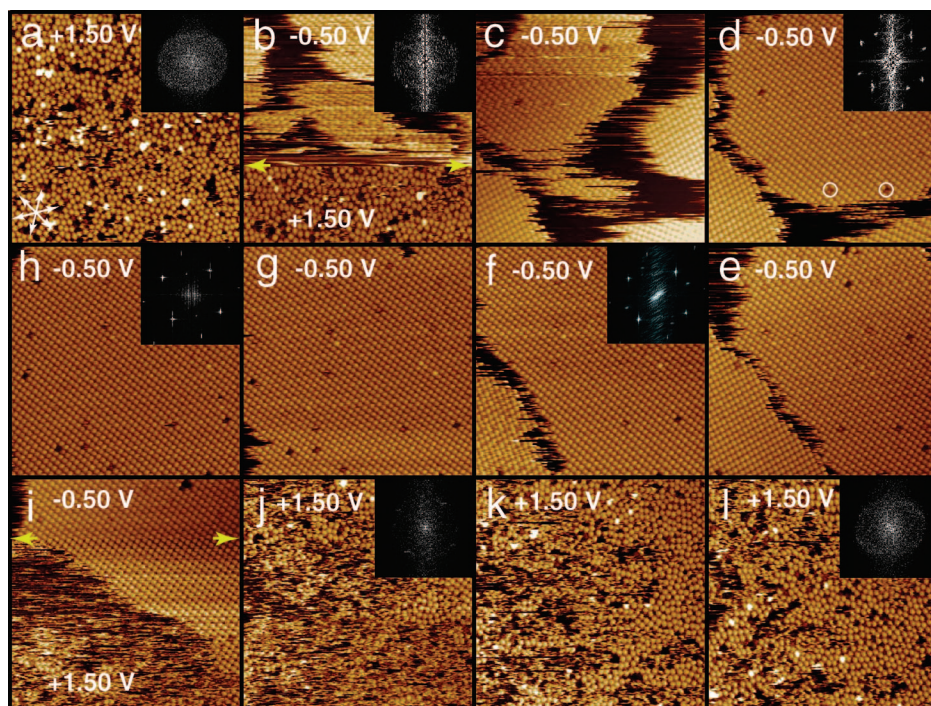


**Figure 4.** Sequential STM images obtained at the same area illustrating the bias induced phase transition. The time interval between images is 34 s. At the beginning, bias is set to 1.50 V (tunneling current is kept to 362 pA through out the process). At the place marked by the yellow arrows in image b, the bias was suddenly changed to  $-0.50$  V. The change of tip bias immediately induced a disorder to order phase transition in the assembling layer. During the scanning under this negative bias, a consecutive growth of the 4-fold crystal domains could be clearly observed (c to h). All of the differently orientated domains join the largest domain in the upper left of image c to form a single domain. The two white circles mark two defects in the crystal domain keep nearly unchanged in the growing process. This enables us to see the growing process more clearly. In image i, the bias changed back to 1.50 V at the place marked by the arrows, this immediately induce destabilization of the crystal domain, and the assembling layer finally becomes an amorphous layer lacking long-range order (image i to l). In the lower left of image a, the three main directions of the graphite substrate are indicated by the white arrows.

could also serve as an indication of different orientation of the molecules under different bias polarities.

The field induced orientational response of **cpd 1** is schematically illustrated in Figure 3c. The extra stability energy  $E_{\text{energy}}$  caused by the interaction between the intrinsic molecular dipole  $\vec{P}$  and the applied electric field  $\vec{E}_{\text{energy}}$  could be calculated with the equation  $E_{\text{energy}} = -\vec{P} \cdot \vec{E}_{\text{external}}$ . If the distance between the STM tip and the substrate surface is assumed to be 1 nm,<sup>20</sup> the interaction between the molecular dipole and the external electric field could be calculated to be around 0.30 to 0.56 eV (with an applied bias ranging from  $\pm 0.80$  V to  $\pm 1.50$  V). In comparison with the thermal energy  $kT$  at room temperature (about 0.03 eV), this energy is significant and is considered sufficient to induce flipping of the molecule in the electric field.

We wish to note that the solvent, 1-phenyloctane, used in this work is a typical nonpolar solvent. Currently, we do not see the possibility of significant influence of solvent polarity on the phase transition characteristics under different bias. The solvent can be considered as a dielectric medium in the tunneling junction, and the dielectric constant of this medium may influence the strength of electric field felt by the molecules. However, the dielectric constant should be independent of the bias polarity and intensity. Whereas if different solvents are used, it is possible that the critical electric field needed for phase transition could be affected by the solvent polarity/dielectric constant.

Another point worth noting is the possibility of STM tip manipulation. The typical imaging conditions in the current study are operated with a rather large tunneling resistance,  $G\Omega$  range, which is significantly higher than typical contact resistance in STM studies,<sup>21</sup> and means the tip should be in the van der Waals interaction rather than the repulsive interaction regime that is pertinent to molecular manipulations. Thus, STM tip manipulation effect is considered negligible in our study.<sup>22</sup> This consideration is further supported in the parallel studies by changing the bias (without changing polarity) or tunneling current to tune the tip–substrate distance. There was no evidence of induced phase transition in such parallel observations.

A significant difference of the field induced flipping of this sandwich complex from the nonplanar SnPc where the ordering of the assembly remains after flipping is that the ordering of the assembling structures is changed completely after molecule flip. This is considered to be due to the significant difference in the assembling characteristics between  $Pc(15C5)_4$  and  $PcOC8$  moieties. To further understand the bias induced phase transition of this noncentrosymmetric complex, the assembling of another triple-decker sandwich complex, **cpd 2** was studied. In contrast to the noncentrosymmetric molecular structure of **cpd 1**, this compound has a centrosymmetric structure, and no intrinsic dipole is expected. This compound exhibits disordered structures under both positive and negative bias, with an average intermo-

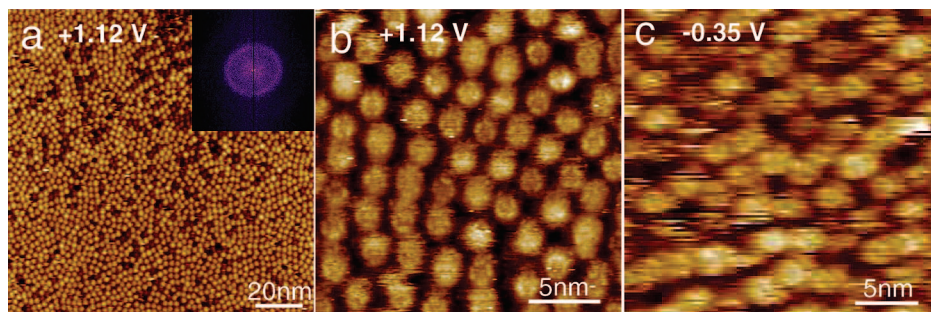


**Figure 5.** STM image of the amorphous assembly of **cpd 2** at the 1-phenyloctane/graphite interface obtained with positive (a,b) and negative (c) bias. Imaging condition: bias 1.12 V, tunneling current 193 pA (a) and 347 pA (b), bias  $-0.35$  V, tunneling current 695 pA (c).

lecular distance of about 2.6 nm (Figure 5). Since the PcOC8 moiety is in the center of this molecule, the octyloxy chains do not form sufficient interdigitation and result in a disordered arrangement. Similar to **cpd 1**, submolecular resolution could also be obtained. The molecules could be distinguished to be randomly orientated in the assembly. Eight bright spots could be identified for each molecule and could be attributed to the four peripheral phenyl rings. The diameter of each molecule is estimated to be about 1.6 nm, the same as that of the noncentrosymmetric complex. In comparison with CuPcOC8, the peripheral phenyl rings of the Pc moiety appear with higher contrast in the STM image than the inner part, which is possibly due to the nonplanar conformation of the top Pc ring. The result on this centrosymmetrical sandwich molecule further confirms that the interaction between the intrinsic molecular dipole of the noncentrosymmetric **cpd 1** with the electric field is the main cause of the bias induced phase transition.

To summarize, a strategy has been proposed for controlling the assembling conformation of organic molecules at the liquid/solid interface by external electric field. Two triple-decker sandwich complexes with noncentrosymmetric and centrosymmetric structure have been designed and synthesized to validate this strategy. As expected, the noncentrosymmetrical sandwich molecule with intrinsic molecular dipole shows reversible phase transition to the change of bias polarity. Under negative bias, the noncentrosymmetrical **cpd 1** forms ordered assembly, which is a “hetero-chiral” mixture of two pseudochiral isomers resulting from the twisting of Pc ligands, while under positive bias a disordered assembly is revealed. The difference in polarity and assembling properties of the top and bottom Pc ligands result in different responding speed of the molecule to different bias polarities. The control experiment on a centrosymmetrical sandwich molecule confirms that the interaction between the intrinsic molecular dipole of the noncentrosymmetrical triple-decker molecule and the external electric field is responsible for this field induced phase transition. Since the electronic properties of single molecules as well as thin films of such organic molecules are directly related to the ordering of the molecules, our results provide a possible route for controlling the ordering, orientation, and possibly electronic and interface

properties (such as wettability) of the organic species by external field and is of genuine relevance to the conceptual bottom-up approach of constructing functional molecular architectures.<sup>22,23</sup>

**Acknowledgment.** The authors are grateful for the financial support from National Natural Science Foundation (Grants 50573089, 90406024, 20325105, and 20431010) and the Knowledge Innovation Program of the Chinese Academy of Sciences (Grant KJCX2-YW-M04).

**Supporting Information Available:** Elemental analysis, STM images, definition and statistics of the azimuthal angle, schematic of the triple-decker sandwich molecule. This material is available free of charge via the Internet at <http://pubs.acs.org>.

## References

- (1) (a) Bao, Z.; Lovinger, A.-J.; Dodabalapur, A. *Appl. Phys. Lett.* **1996**, *69*, 3066. (b) Bao, Z.; Lovinger, A.-J.; Brown, J. *J. Am. Chem. Soc.* **1998**, *120*, 207.
- (2) Nicholson, M. M. In *Phthalocyanines—Properties and Applications*, Vol. 3; Leznoff, C.-C., Lever, A.-B.-P., Eds.; VCH: New York, 1993; pp 71–117.
- (3) (a) Chen, Y.; Su, W.; Bai, M.; Jiang, J.; Li, X.; Liu, Y.; Wang, L.; Wang, S. *J. Am. Chem. Soc.* **2005**, *127*, 15700. (b) Madru, R.; Guillaud, G.; Al Sadoun, M.; Maitrot, M.; André, J.-J.; Simon, J.; Even, R. *Chem. Phys. Lett.* **1988**, *145*, 343. (c) Clarisse, C.; Riou, M.-T.; Gauneau, M.; Le Contellec, M. *Electron. Lett.* **1988**, *24*, 674. (d) Guillaud, G.; Al Sadoun, M.; Maitrot, M.; Simon, J.; Bouvet, M. *Chem. Phys. Lett.* **1990**, *167*, 503. (e) Su, W.; Jiang, J.; Xiao, K.; Chen, Y.; Zhao, Q.; Yu, G.; Liu, Y. *Langmuir* **2005**, *21*, 6527.
- (4) (a) Souto, J.; Rodríguez, M. L.; Desaja, J. A.; Aroca, R. *Int. J. Electron. B* **1994**, *76*, 763. (b) Bassoul, P.; Toupance, T.; Simon, J. *Sens. Actuators. B* **1995**, *26–27*, 150. (c) Rickwood, K. R.; Lovett, D. R.; Lukas, B.; Silver, J. *J. Mater. Chem.* **1995**, *5*, 725. (d) Liang, B.; Yuan, C.; Wei, Y.; Zhang, Y.; Jiang, D.; Zhang, S.; Lu, A. *Synth. Met.* **1997**, *88*, 219. (e) Álvarez, J.; Souto, J.; Rodríguez-Méndez, M. L.; de Saja, J. A. *Sens. Actuators B* **1998**, *48*, 339.
- (5) (a) Shinkai, S.; Ikeda, M.; Sugasaki, A.; Takeuchi, M. *Acc. Chem. Res.* **2001**, *34*, 494. (b) Sugasaki, A.; Ikeda, M.; Takeuchi, M.; Robertson, A.; Shinkai, S. *J. Chem. Soc., Perkin Trans.* **1999**, *1*, 3259.
- (6) Tashiro, K.; Konishi, K.; Aida, T. *J. Am. Chem. Soc.* **2000**, *122*, 7921.
- (7) Kay, E. R.; Leigh, D. A.; Zerbetto, F. *Angew. Chem., Int. Ed.* **2007**, *46*, 72.
- (8) (a) Hodgson, M. J.; Borovkov, V. V.; Inoue, Y.; Arnold, D. P. *J. Organomet. Chem.* **2006**, *691*, 2162. (b) Monti, D.; Cantonetti, V.; Venanzi, M.; Ceccacci, F.; Bombelli, C.; Mancini, G. *Chem. Commun.* **2004**, 972. (c) Caselli, A.; Gallo, E.; Ragaini, F.; Ricatto, F.; Abbiati, G.; Cenini, S. *Inorg. Chim. Acta* **2006**, *359*, 2924. (d) Adachi, K.; Chayama, K.; Watarai, H. *Langmuir* **2006**, *22*, 1630. (e) Muto, T.; Sassa, T.; Wada, T.; Kimura, M.; Shirai, H. *Chem. Lett.* **2004**, *33*, 132.



- (9) Bian, Y.; Wang, R.; Wang, D.; Zhu, P.; Li, R.; Dou, J.; Liu, W.; Choi, C.; Chan, H.; Ma, C.; Ng, D. K. P.; Jiang, J. *Helv. Chim. Acta* **2004**, 87, 2581.
- (10) (a) Stepanow, S.; Lin, N.; Vidal, F.; Landa, A.; Ruben, M.; Barth, J. V.; Kern, K. *Nano Lett.* **2005**, 5, 901. (b) Gesquiere, A.; Jonkheijm, P.; Hoebe, F. J. M.; Schenning, A. P. H. J.; De Feyter, S.; De Schryver, F. C.; Meijer, E. W. *Nano Lett.* **2004**, 4, 1175. (c) Yablon, D. G.; Wintgens, D.; Flynn, G. W. *J. Phys. Chem. B* **2002**, 106, 5470. (d) Brian, C.; Parkinson, B. A. *J. Am. Chem. Soc.* **2003**, 125, 12712. (e) Xu, Q. M.; Wang, D.; Wan, L. J.; Wang, C.; Bai, C. L.; Feng, G. Q.; Wang, M. X. *Angew. Chem., Int. Ed.* **2002**, 41, 3408.
- (11) (a) Klymchenko, A. S.; Slevin, J.; Binnemans, K.; De Feyter, S. *Langmuir* **2006**, 22, 723. (b) Binnemans, K.; Slevin, J.; De Feyter, S.; De Schryver, F. C.; Donnio, B.; Guillon, D. *Chem. Mater.* **2003**, 15, 3930. (c) Yang, Z. Y.; Gan, L. H.; Lei, S. B.; Wan, L. J.; Wang, C.; Jiang, J. Z. *J. Phys. Chem. B* **2005**, 109, 19859. (d) Ma, H.; Ou Yang, L. Y.; Pan, N.; Yau, S. L.; Jiang, J.; Itaya, K. *Langmuir* **2006**, 22, 2105. (e) Takami, T.; Arnold, D. P.; Fuchs, A. V.; Will, G. D.; Goh, R.; Waclawik, E. R.; Bell, J. M.; Weiss, P. S.; Sugiura, K.; Liu, W.; Jiang, J. *J. Phys. Chem. B* **2006**, 110, 1661.
- (12) Yang, Y. L.; Chan, Q. L.; Ma, X. J.; Deng, K.; Shen, Y. T.; Feng, X. Z.; Wang, C. *Angew. Chem., Int. Ed.* **2006**, 45, 6889.
- (13) (a) For synthesis and characterizations of these sandwich complexes see Jiang, J.; Bian, Y.; Furuya, F.; Liu, W.; Choi, M. T. M.; Kobayashi, N.; Li, H. W.; Yang, Q.; Mak, T. C. W.; Ng, D. K. P. *Chem. Eur. J.* **2001**, 7, 5059. (b) Zhu, P.; Pan, N.; Li, R.; Dou, J.; Zhang, Y.; Cheng, D. Y. Y.; Wang, D.; Ng, D. K. P.; Jiang, J. *Chem. Eur. J.* **2005**, 11, 1425. (c) Bian, Y.; Li, L.; Wang, D.; Choi, C.; Cheng, D. Y. Y.; Zhu, P.; Li, R.; Dou, J.; Wang, R.; Pan, N.; Ng, D. K. P.; Kobayashi, N.; Jiang, J. *Eur. J. Inorg. Chem.* **2005**, 2612. (d) Tashiro, K.; Konishi, K.; Aida, T. *J. Am. Chem. Soc.* **2000**, 122, 7921. and also Supporting Information.
- (14) Perdew, J. P.; Wang, Y. *Phys. Rev. B* **1992**, 45, 13244.
- (15) Gopakumar, T. G.; Müller, F.; Hietschold, M. *J. Phys. Chem. B* **2006**, 110, 6051.
- (16) (a) Qiu, X.; Wang, C.; Zeng, Q.; Xu, B.; Yin, S.; Wang, H.; Xu, S.; Bai, C. *J. Am. Chem. Soc.* **2000**, 122, 5550. (b) Qiu, X.; Wang, C.; Yin, S.; Zeng, Q.; Xu, B.; Bai, C. *J. Phys. Chem. B* **2000**, 104, 3570.
- (17) Hooks, D. E.; Fritz, T.; Ward, M. D. *Adv. Mater.* **2001**, 13, 227.
- (18) (a) Ye, T.; Takami, T.; Wang, R.; Jiang, J.; Weiss, P. S. *J. Am. Chem. Soc.* **2006**, 128, 10984. (b) Yoshimoto, S.; Sawaguchi, T.; Su, W.; Jiang, J. Z.; Kobayashi, N. *Angew. Chem. Int. Ed.* **2007**, 46, 1071.
- (19) Sheng, N.; Li, R.; Choi, C. F.; Su, W.; Ng, D. K. P.; Cui, X.; Yoshida, K.; Kobayashi, N.; Jiang, J. *Inorg. Chem.* **2006**, 45, 3794.
- (20) (a) Note here the 1 nm tip-sample distance is only an approximate assumption, the tip-sample distance will change when the bias voltage is changed: in general, smaller bias corresponds to a smaller tip-sample distance. However, according to the exponential dependence of tunneling current with tip-sample distance,  $I \propto V \exp(-d \sqrt{\Phi})$ , we do not expect large change in the tip-sample distance when the bias changes between 800 mV to 1.5 V. It should also be noted that we have made no effort in quantitatively determining the tip-substrate distance. The determination of tip-sample distance has been extensively pursued both theoretically and experimentally, and the tip-sample distances are generally believed to be in the range of a few angstroms to around 1 nm [for example, see Tersoff, J.; Hamann, D. R. *Phys. Rev. B* **1985**, 31, 8051. (b) Lang, N. D. *Phys. Rev. B* **1986**, 34, 5947. (c) Lang, N. D. *Phys. Rev. B* **1988**, 37, 10395.]
- (21) (a) Joachim, C.; Gimzewski, J. K.; Schlittler, R. S.; Chavy, C. *Phys. Rev. Lett.* **1995**, 74, 2102, for example. (b) Gimzewski, J. K.; Joachim, C. *Science* **1999**, 283, 1683.
- (22) Weigelt, S.; Busse, C.; Petersen, L.; Rauls, E.; Hammer, B.; Gothelf, K. V.; Besenbacher, F.; Linderoth, T. R. *Nat. Mater.* **2006**, 5, 112.
- (23) Otero, R.; Hümmelink, F.; Sato, F.; Legoas, S. B.; Thosttrup, P.; Lægsgaard, E.; Stensgaard, I.; Galvão, D. S.; Besenbacher, F. *Nat. Mater.* **2004**, 3, 779.

NL0803186